

NMR Structure of PW2 Bound to SDS Micelles

A TRYPTOPHAN-RICH ANTICOCCIDIAL PEPTIDE SELECTED FROM PHAGE DISPLAY LIBRARIES*

Received for publication, April 30, 2002, and in revised form, July 1, 2002
Published, JBC Papers in Press, July 18, 2002, DOI 10.1074/jbc.M204225200

Luzineide W. Tinoco‡, Arnaldo da Silva, Jr.§, Adilson Leite§, Ana Paula Valente‡¶, and Fabio C. L. Almeida‡¶

From the ‡Centro Nacional de Ressonância Magnética Nuclear, Departamento de Bioquímica Médica – Instituto de Ciencias Biomedicas, Universidade Federal do Rio de Janeiro, 21941-590 – Rio de Janeiro, RJ, Brazil and the §Centro de Biologia Molecular e Engenharia Genética, Universidade Estadual de Campinas, 23083-970 – Campinas, SP, Brazil

PW2 (HPLKQYWWRPSI) was selected from phage display libraries through an alternative panning method using living sporozoites of *Eimeria acervulina* as target. Synthetic PW2 shows anticoccidial activity against *E. acervulina* and *Eimeria tenella* with very low hemolytic activity. It also displays antifungal activity but no activity against bacteria. We present the solution structure of the PW2 bound to SDS micelles. In the absence of an interface, PW2 is in random coil conformation. In micelles, structural calculation shows that Trp-7 forms the hydrophobic core that is important for the peptide folding. Lys-4, Tyr-6, Trp-8, and Arg-9 are in the same surface, possibly facing the micelle interface. This possibility was supported by the fact that chemical shift differences for these residues were more pronounced when compared with PW2 in water and in SDS. PW2 gains structure upon binding to SDS micelles. Lys-4, Tyr-6, Trp-8, and Arg-9 were found to bind to the micelle. Trp-7, Trp-8, and Arg-9 composed the WW+ consensus found in the sequence of the peptides selected with the phage display technique against *E. acervulina* sporozoites. This suggested that Trp-7, Trp-8, and Arg-9 are probably key residues not only for the peptide interaction with SDS micelles but also for the interaction with *E. acervulina* sporozoites surface.

The presence of antimicrobial peptides in the animal and plant kingdoms suggests that these molecules played a fundamental role in the evolution of complex multicellular organisms. There are a large number of antimicrobial peptides with considerable sequence diversity. Rarely, the same peptide sequence is recovered from two different species, even those closely related, such as insects, frogs, or mammals. Exceptions include peptides cleaved from highly conserved proteins, such as buforin II (1).

The novel anticoccidial peptide PW2 (HPLKQYWWRPSI)

was selected from phage display peptide libraries by an alternative method of panning using living *Eimeria acervulina* sporozoites as targets. PW2 was also effective against *Eimeria tenella* and several other fungi. It showed low activity against *Toxoplasma gondii* tachyzoites and no activity against *Trypanosoma cruzi*, *Crithidia fasciculata* epimastigotes, or bacteria. In addition, the parasitocidal concentrations of PW2 produced very low lytic effects on mammalian and avian cells (2).

PW2 is a Trp-rich peptide with antimicrobial activity. Several other Trp-rich peptides presenting antimicrobial activity are described in the literature. Indolicidin (ILPWKWPWWP-WRR, Refs. 3–6) and tritripticin (VRRFPWWPFLRR, Refs. 7) are Trp-rich peptides obtained from neutrophils with antibacterial and antifungal activity. Their structures were solved in solution in the presence of micellar interfaces (8, 9). Other Trp-rich antimicrobial peptides have been described in the literature: ACE-AMP1 (10) is a lipid transfer protein, and puroindolins A and B are wheat plant defensins stabilized by disulfide bridges (11).

PW2 disrupts the sporozoite pellicle possibly through membrane permeabilization (2) in the same manner as other Trp-rich peptides with antimicrobial activity, such as indolicidin (12) and tritripticin (9). However, the detailed mechanism of action of antimicrobial peptides remains to be elucidated. A model that explains the activity of most antimicrobial peptides is the Shai-Matsuzaki-Huang model (13–15), which proposes the initial interaction of the peptide with the membrane followed by displacement of lipids, alteration of membrane structure, and in certain cases, entry of the peptide into the target cell.

Several studies suggested that membrane perturbation is an important, but not a lethal, event. These studies have proposed that the initial step is an electrostatic association of the positively charged peptide with the negatively charged groups of the membrane. This association would be followed by peptide folding into amphipathic structures. Consequently, this interaction would distort the outer membrane bilayer, allowing access to the cytoplasmic membrane, where peptide channel formation is thought to occur (16–19). There is a growing body of evidence indicating that antimicrobial peptides may not solely kill by membrane disruption but may follow various mechanisms of action, including their interaction with cellular targets (13, 14, 20–22).

In a study with indolicidin, a 13-residue Trp-rich peptide from bovine neutrophils, it was found that antibacterial activity was not due to membrane permeabilization (16). Substitution of the tryptophans by phenylalanine and prolines by alanines did not suppress antimicrobial activity (16). The preponderance of aromatic residues and the overall cationic nature might favor interaction with nucleic acids. It is conceivable that indolicidin might exert its activity by interacting

* This work was supported by the Brazilian financial agencies: Conselho Nacional de Desenvolvimento Científico e Tecnológico, PRONEX (Programa de Apoio a Núcleos de Excelência), Fundação Universitária José Bonifácio and Fundação de Amparo à Pesquisa do Estado de São Paulo. The costs of publication of this article were defrayed in part by the payment of page charges. This article must therefore be hereby marked “advertisement” in accordance with 18 U.S.C. Section 1734 solely to indicate this fact.

The atomic coordinates and structure factors (code 1M02) have been deposited in the Protein Data Bank, Research Collaboratory for Structural Bioinformatics, Rutgers University, New Brunswick, NJ (<http://www.rcsb.org/>).

¶ To whom correspondence may be addressed. Tel.: 5521-25626756; Fax: 5521-22708647; E-mail: valente@cnrmn.bioqmed.ufjr.br or falmeida@cnrmn.biogmed.ufjr.br.

with nucleic acids, thus preventing both replication and/or transcription (8).

In the present manuscript, we present the solution structure of PW2 bound to membrane-mimetic SDS micelles by two-dimensional NMR methods. PW2 was also fully assigned in water, 40 mM SDS, and 160 mM SDS. Chemical shift comparison enabled us to assign the possible site of interaction with the interface of the micelles. This study contributes to the elucidation of the mechanism of peptide-membrane interactions and highlights several structural features that are important for this interaction.

EXPERIMENTAL PROCEDURES

CD Spectroscopy—CD measurements were taken on a Jasco J-715 CD spectrophotometer with a 2-mm path length cell cuvette. The wavelengths, from 190 to 260 nm, were measured with a 1-nm step resolution, a 50-nm/min sweep speed, an 8-s response time, and a 1-nm bandwidth. All the spectra were collected and averaged over four scans at room temperature. The samples of PW2 (63 μ M) were prepared in 20 mM sodium phosphate buffer (pH 5.0 and 7.2). SDS (2–40 mM) and TFE¹ (10–75%) were added to the PW2 sample. No solvent spectral subtraction was performed.

NMR Spectroscopy—The NMR samples were prepared by adding solutions of SDS-*d*₂₅ (Cambridge Isotope Laboratories, Andover, MA) in 20 mM sodium phosphate buffer (pH 5.0) containing 100 mM sodium chloride, 10% D₂O (99.9%, Isotec, Inc.) to lyophilized PW2. The final samples were 4 mM in PW2 and 30–160 mM in SDS-*d*₂₅. NMR spectra were recorded on a Bruker Avance DRX600 or DRX400 operating at 600.04 or 400.13 MHz, respectively. The sample temperature was maintained at 25 °C. TOCSY spectra (spin-lock time of 70 ms) were acquired using the MLEV-17 pulse sequence (23). NOESY spectra (24) were acquired using a 75-ms mixing time. Water suppression was achieved using the WATERGATE technique (25), and the spectra were collected with 512 data points in F1 and 4096 data points in F2 with 16 transients. The NMR data were processed with NMRPIPE (26). Resolution enhancement was achieved by apodization of the free induction decay with exponential multiplication and zero filling.

NMR Data Analysis and Structure Calculation—All NMR spectra were analyzed using NMRVIEW, version 4.1.2 (27). NOE cross-peaks were integrated in the NOESY spectra, and their volumes were converted to distances, which were calibrated using the equations suggested by Hyberts *et al.* (28). No stereospecific assignments were made. No hydrogen bonds were applied. The structure calculations were performed using CNS_Solve version 1.1 (29). Starting with the extended structure, 100 structures were generated using simulated annealing protocol. This was followed by 10,000 steps of simulated annealing at 1000 K and a subsequent decrease in the temperature in 20,000 steps in the first slow-cool annealing stage. All the structures were analyzed with the program MOLMOL (30).

RESULTS

We selected three sample conditions to perform the resonance assignments of PW2. The first was in water (20 mM sodium phosphate buffer, pH 5.0) and was used for comparison with the other experimental conditions, being representative of the free state in solution. In the other two conditions, the samples were in the presence of 40 and 160 mM SDS, respectively. The behavior of PW2 in the presence of detergents was intriguing. In the absence of SDS, the peptide was highly soluble. At SDS/PW2 molar ratios lower than 7.5, PW2 precipitates. When the relative amount of SDS was raised further, PW2 became soluble again. A similar behavior has been reported for indolicidin (8). We chose to work using two SDS/PW2 molar ratios in which PW2 was soluble. At a high molar ratio, little conformational exchange was observed (Fig. 1), mainly because PW2 was preferentially bound to the interface. Under those conditions, we obtained good quality spectra, and the assignment was straightforward. On the other hand, at [SDS]/

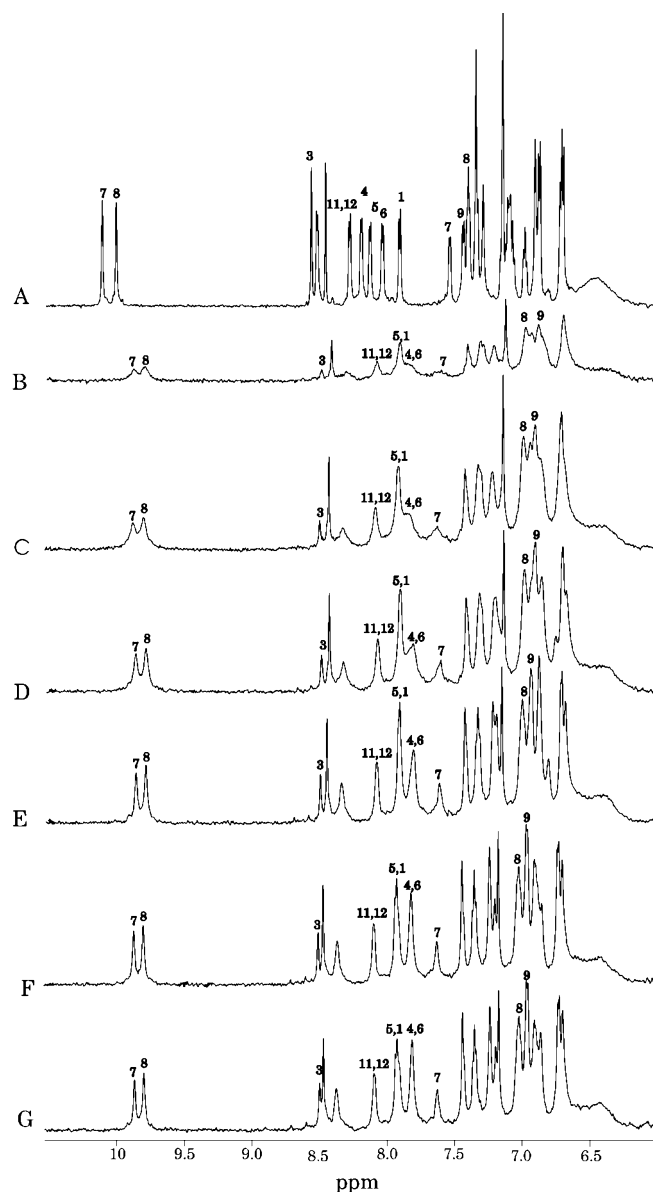


FIG. 1. Amidic and aromatic region of the ¹H one-dimensional NMR spectra of PW2 (4 mM) at 25 °C. A, 20 mM sodium phosphate buffer at pH 5.0; B, 30 mM SDS ([SDS]/[PW2] = 7.5); C, 40 mM SDS ([SDS]/[PW2] = 10); D, 50 mM SDS ([SDS]/[PW2] = 12.5); E, 80 mM SDS ([SDS]/[PW2] = 20); F, 120 mM SDS ([SDS]/[PW2] = 30); G, 160 mM SDS ([SDS]/[PW2] = 40).

[PW2] = 10, there was considerable conformational exchange, as evidenced by the broader spectral lines (Fig. 1). The TOCSY spectrum was uninformative, due to fast relaxation during the spin-lock time (small $T_{1\rho}$).

The conformational exchange when [SDS]/[PW2] = 10 could be explained by a millisecond to microseconds time scale equilibrium between the free and micelle-bound states of PW2. Fig. 1 shows the one-dimensional hydrogen spectrum of PW2 as a function of SDS concentration. Note that the spectrum in water displays sharp lines (Fig. 1A). Upon addition of SDS, there was an increase in line width (Fig. 1, B and C), indicating the presence of conformational exchange. By ignoring the line width differences, the two conditions in SDS showed very similar profiles, indicating similar structures for PW2. [SDS]/[PW2] = 10 was representative of an intermediate step in the binding process, whereas the [SDS]/[PW2] = 40 ratio was considered as the bound state.

CD Spectroscopy—The CD spectra of PW2 recorded with and

¹ The abbreviations used are: TFE, trifluoroethanol; NOE, nuclear Overhauser effect; NOESY, NOE spectroscopy; TOCSY, total correlation spectroscopy; r.m.s.d., root mean square deviation.

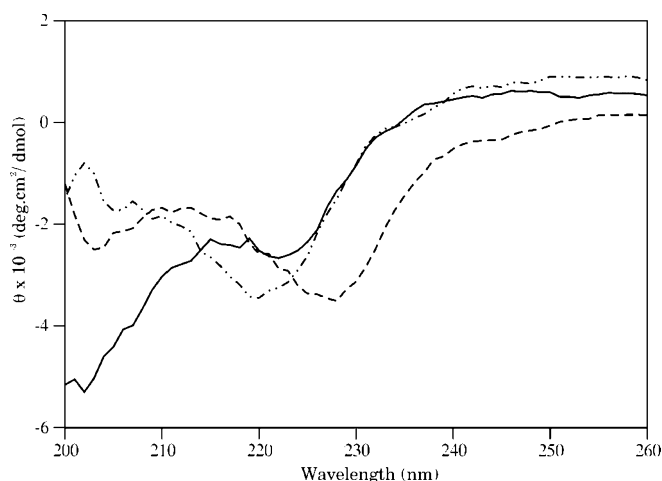


FIG. 2. Circular dichroism spectra of PW2 63 μM in 20 mM sodium phosphate buffer at pH 5.0 and 25 $^{\circ}\text{C}$. Solid line, only buffer; dashed line, buffer and 4 mM SDS; dashed dotted line, buffer and 25% TFE.

without SDS and TFE are shown in Fig. 2. In aqueous solution, the spectrum presents a negative band at 200 nm (-5000 degrees $\text{cm}^2 \text{dmol}^{-1}$). This is typical of peptides in a random coil conformation (31) and corroborates the data in Fig. 1. The addition of 25% TFE and SDS led to a gain of structure. This is supported by the fact that the negative band at 200 nm became less negative and more intense between 200 and 230 nm. An intense negative band at 220 nm was observed in the presence of 25% TFE (220 nm) and 4 mM SDS (228 nm). These negative bands at ~ 225 nm are characteristic features of aromatic bundles (31) or turns in the structure (32). The bands arising from the excitation of aromatic rings can be either positive or negative. The negative band at 220 nm observed in 25% TFE was not necessarily typical of a helical structure because there were no negative band at 208 nm at this condition. The CD analysis of the secondary structures in these spectra is complex since the presence of the aromatic side chains prevents the observation of the secondary structure characteristic bands. CD spectroscopy was in complete agreement with Fig. 1. CD spectra do not change significantly when the SDS/PW2 molar ratios are increased above 7.5.

Chemical shift assignments—The chemical shift assignments of PW2 in 20 mM sodium phosphate buffer (pH 5.0) and in SDS (40 and 160 mM) were performed by the sequential strategy as proposed by Wüthrich (33). Sequential connectivities could be observed through $d\alpha N(i+1)$, $d\beta N(i+1)$, and $dNN(i+1)$ NOEs.

Structure Calculation—The structure calculation was performed with distance restraints obtained at the molar ratio [SDS]/[PW2] equal to 40. Structural statistics are shown in Table I. A total of 154 NOEs were unambiguously identified, being 50 inter-residual NOEs. There are two spin systems for proline 2 δ -hydrogens, indicative of the existence of *cis* and *trans* conformations for this amino acid. The $d\alpha\delta(i+1)$ NOE, typical for the *trans* conformer of proline, and the $d\alpha\alpha(i+1)$ NOE, typical of the *cis* conformer of proline, were not observed for Pro-2 (33); therefore, we could not unambiguously identify the *cis* and *trans* conformers. Probably the absence of these NOEs was due to the high flexibility of the N terminus of PW2. In the case of Pro-10, only $d\alpha\delta(i+1)$ NOEs were observed, indicating that this proline is in *trans* conformation. Clearly, Pro-10 is in a more structured portion of the polypeptide chain.

Long range NOEs between the side chain $\text{H}\epsilon_3$ tryptophan 7 and the δ - and γ -hydrogens of Pro-2 were observed. These non-ambiguous NOEs were important in defining the folding of

the peptide. It is important to mention that both proline 2 spin systems present these long range NOEs connecting to Trp-7. Other long range NOEs were responsible for a well defined three-dimensional structure of the peptide: Tyr-6($\text{H}\epsilon$) with Leu-3($\text{H}\delta$), Tyr-6($\text{H}\delta$) with Leu-3($\text{H}\alpha$), Trp-7($\text{H}\epsilon$) with Ser-11($\text{H}\alpha$), among others. Table I shows the list of all medium and long range NOEs.

The NOESY spectrum in water presented only intraresidual and sequential NOEs, indicating lack of structure under those conditions. The assignment was straightforward due the relatively sharp lines and the good quality of the spectra (not shown).

The NOESY spectrum of PW2 at the SDS/PW2 molar ratio of 10 presented three spin systems for Leu-3 as a consequence of its vicinity to Pro-2, which undergoes slow exchange between the *cis* and *trans* conformations. With the increase of the [SDS]/[PW2] molar ratio to 40, the number of Leu-3 spin systems decreased to two, indicating a conformational stabilization of the peptide. The two spin systems for Leu-3 were identical by considering the NOEs present in each of them. The calculated structure is shown in Fig. 3. Fig. 3A shows the superposition of the 20 lowest energy structures, and Fig. 3B shows the lowest energy structure. The peptide is folded in such a way that tryptophan 7 forms a hydrophobic core along with proline 2 and proline 10. The aromatic residues tyrosine 6 and tryptophan 8 are exposed to the surface of the peptide and could, therefore, be the responsible for the negative band at ~ 225 nm observed in the CD spectra. The presence of two turns that characterize the structure could also give rise to the negative band observed in the CD spectra. Both aromatic residues are in the vicinity of the positively charged amino acids, arginine 9 and lysine 4. The close proximity of the side chain of Trp-9 and Arg-9 is suggestive of a π -stacking interaction that could contribute to the stabilization of the whole three-dimensional conformation.

Fig. 3C shows the electrostatic surface plot of the lowest energy structure. The structure has a triangular shape whose base could be postulated as the contact surface with the micelle interface. The solution structure suggests that the peptide folds so that the aromatic residues and the positively charged amino acids form a flat surface. This surface extends from Lys-4 to Arg-9.

Fig. 4, A and B, shows the comparison of the α and the amide hydrogen chemical shifts of PW2 in buffer, [SDS]/[PW2] = 10 and [SDS]/[PW2] = 40 with the random coil values (33). In the presence of SDS, there is a pronounced amide chemical shift change from residues Lys-4 to Arg-9. For α -hydrogens, the difference in chemical shifts behave in a similar way. In both SDS/PW2 molar ratios, chemical shift differences are similar except for residues Trp-8 and Arg-9. Chemical shift differences between random coil values and the three conditions used show the same profile. This was important since it indicates that, in the absence of SDS (free state), PW2 might show the same structural tendency observed in SDS but with more flexibility.

Although with a similar profile, PW2 chemical shifts differ between the free state and the SDS bound state at different SDS/PW2 molar ratios (Fig. 4, C and D). The largest positive differences for the α -hydrogens (Fig. 4D) were observed for residues Lys-4, Gln-5, Tyr-6, Trp-7, Trp-8, and Arg-9. A negative chemical shift difference was observed for residue Ile-12. For the amidic hydrogens (Fig. 4C), the most pronounced chemical shift differences occurred in residues Lys-4, Gln-5, Tyr-6, Trp-8, Arg-9, Ser-11, and Ile-12. The two SDS/PW2 molar ratios studied behave similarly for most of the residues with the exception of Trp-8 and Trp-9 (Fig. 4C).

These chemical shift differences (Fig. 4, C and D) reflected the process of PW2 binding to the micelle interface. The residues that showed more striking chemical shift changes were

TABLE I
Summary of structural statistics for PW2 in SDS micelles

Total no. of distance constraints	154
No. of intraresidue constraints	104
No. of sequential constraints	39
No. of medium to long range constraints	11
List of the medium to long range NOEs	
i, i+2: Lys-4(H _N) -Pro-2(H α), Trp-7(H _N) -Gln-5(H β), Leu-3(H δ)-Gln-5(H _N), Trp-8(H _N) -Pro-10(H γ), Lys-4(H _N) -Pro-2(H β)	
i, i+3: Tyr-6(H ϵ)-Leu-3(H δ), Tyr-6(H δ)-Leu-3(H δ), Tyr-6(H δ)-Leu-3(H α)	
i, i+4: Trp-7(H ϵ 3) -Ser-11(H α)	
i, i+(>4): Trp-7(H ϵ 3) -Pro-2(H δ), Trp-7(H ϵ 3) -Pro2(H γ)	
r.m.s. deviations from ideal geometry	
covalent bonds (Å°)	0.0024 \pm 0.00030
covalent angles (Å°)	0.5930 \pm 0.0692
improper (degrees)	0.3932 \pm 0.1169
dihedral (degrees)	0.830 \pm 0.01478
NOE	0.0134 \pm 0.0023
Energies (Kcal/mol)	
overall	44.97 \pm 10.96
bond	1.36 \pm 0.34
angle	23.23 \pm 5.19
improper	3.71 \pm 1.93
VDW	11.59 \pm 2.38
NOE	2.75 \pm 1.43
pairwise rmsd (Å)	
residues 1–12	
backbone	1.58
heavy	2.32
residues 4–10	
backbone	0.66
heavy	1.18

Lys-4, Gln-5, Tyr-6, Trp-7, Trp-8, Arg-9, and the C terminus. Residue Trp-7 formed the hydrophobic core of the structure, whereas Lys-4, Tyr-6, Trp-8, and Arg-9 were at the surface. The differences for the amide hydrogens led to the same conclusion with the finding that, for residues Trp-8 and Arg-9, these differences occur only at a SDS/PW2 molar ratio equal to 40. It is noteworthy that chemical shift differences for Trp-8 and Arg-9 between the two SDS/PW2 molar ratios were the only difference between the bound and intermediate state.

Fig. 4, *E* and *F*, shows the number of NOEs and the r.m.s.d. per residue, respectively. It can be observed that there is a higher number of NOEs for residues 6, 7, 8, and 9, in accordance with the residues with higher resolution in the structure. Residues Trp-7, Trp-8, and Arg-9 had the best resolution of them all (lowest r.m.s.d.). These residues also corresponded to the sequence consensus WW+ observed among the peptides selected from phage display libraries using *E. acervulina* sporozoites as target, as reported by Silva, Jr. *et al.* (2).

DISCUSSION

In the present manuscript, we described the solution structure of the peptide PW2 bound to a micelle interface. PW2, selected by phage display, shows anticoccidial activity, being specific for *E. acervulina* and *E. tenella*. It also presents antifungal activity. Although its mode of action is still unknown, membrane permeabilization has been proposed as a possible mechanism of action (2), similarly to other Trp-rich peptides with antimicrobial activity, such as indolicidin (12) and tritrpticin (9).

PW2 displayed some features that were different from the other Trp-rich peptides, such as the absence of antibacterial activity and its low hemolytic activity. One possible explanation is that PW2 has the lowest percentage (50%) of hydrophobic amino acids when compared with indolicidin (77%) and tritrpticin (69%). Studies with indolicidin showed a correlation between the presence of tryptophan residues and hemolytic activity (8). For indolicidin, it was also noted that substitution of tryptophans by phenylalanines decreased the antibacterial

activity but did not eliminate it. Therefore, the low number of tryptophans in PW2 may explain its low hemolytic activity.

Indolicidin, tritrpticin, and PW2 present different antimicrobial activity. Indolicidin has a broad activity spectrum against Gram-positive and Gram-negative bacteria (3), protozoa (4), fungi (5), and the enveloped virus HPV-1 (6). Tritrpticin shows activity against bacteria and fungus (7), and PW2 shows activity against *Eimeria* and fungus (2) but not against bacteria (2). The specificity of Trp-rich peptides is not yet understood. Structural comparison shows an important difference in the positive charge distribution along the peptide chain that might be related to the specificity. For tritrpticin, the positive charges are in the N and C termini of the peptide chain (9). In contrast, in PW2, the two positive charges (Lys-4 and Arg-9) are in the center of the peptide primary structure and close to the aromatic binding region. Indolicidin shows two positive charges in the C terminus and another in the middle of the chain (8).

The observed folding of PW2 is similar to indolicidin (8) and tritrpticin (9). It is noticeable that the multiple tryptophan residues present in these structures tend to form a common structural motif. One tryptophan is part of a hydrophobic core in the structure, whereas other tryptophans are on the surface of the peptide, forming the putative membrane binding site. Prolines and other hydrophobic residues tend to be part of this hydrophobic core.

For PW2, the residues presenting higher chemical shift deviation upon binding to the micelle are Lys-4, Tyr-6, Trp-7, Trp-8, and Arg-9 (Fig. 4). Structural calculation shows that Trp-7 is important for peptide folding, whereas Lys-4, Tyr-6, Trp-8, and Arg-9 are in the same surface, possibly facing the micelle interface. The residues involved in the micelle binding, together with the structural amino acid Trp-7, show the lowest r.m.s.d. for both backbone and side chain.

There was a remarkable chemical shift difference in the amidic hydrogens of residue Trp-8 and Arg-9 between the two SDS concentrations (Fig. 4C). When the SDS/PW2 molar ratio

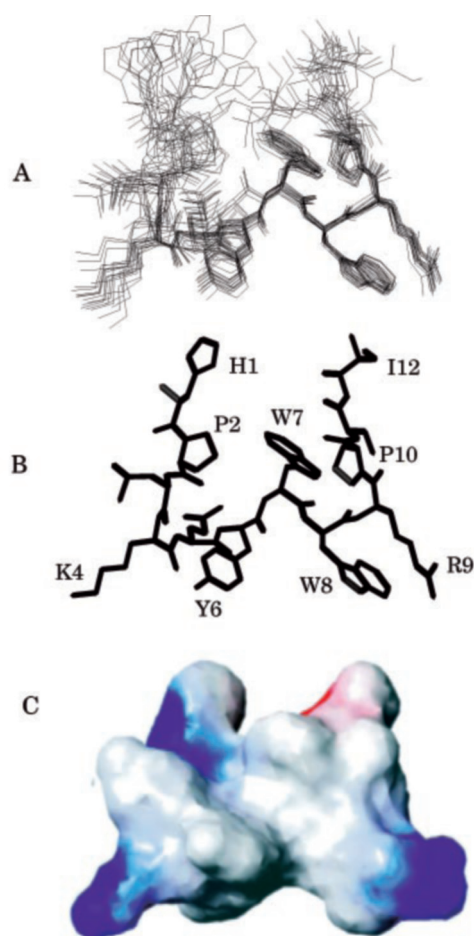


FIG. 3. **Calculated structures for PW2.** A, 20 lowest energy structures calculated for PW2 4 mM in 20 mM sodium phosphate buffer at pH 5.0 and 25 °C with 160 mM SDS-*d*₂₅ showing the well defined region between residues Lys-4 and Pro-10. B and C, lowest energy structure (B) and electrostatic surface plot (C) of the lowest energy structure of PW2. Positive charge is colored in *blue*, neutral charge is colored in *white*, and negative charge is colored in *red*. The figure was generated using the MOLMOL program (30).

varied from 10 to 40, the chemical shifts of Trp-8 and Arg-9 changed in a different way when compared with the other amide peaks. This suggested that Trp-8 and Arg-9 play an important role in the micelle binding process. Electrostatic attraction might constitute the long range force that drives PW2 to the negative SDS micelle interface. Once the peptide is close to the micelle surface, an accommodation of the peptide structure occurs. Chemical shift changes take place at this time, affecting residues Lys-4, Tyr-6, Trp-7, Trp-8, and Arg-9. In the intermediate condition, where SDS/PW2 molar ratio is 10, Trp-8 and Arg-9 could be jumping between the free and bound states, thus explaining the observed conformational exchange. Increasing the SDS concentration (molar ratio SDS/PW2 = 40) decreases the conformational exchange considerably. Possibly, π -stacking interaction between Trp-8 and Arg-9 is formed, thus stabilizing the peptide fold.

It is noteworthy that the positive charge at the Arg-9 position, together with Trp-7 and Trp-8, is the consensus WW+ observed among peptides selected from phage display libraries against living sporozoites of *E. acervulina* (2). This suggests that Trp-7, Trp-8, and Arg-9 are key residues not only for the interaction with SDS micelles but also for the interaction with the *E. acervulina* sporozoites surface.

The sequence consensus WW+, observed in PW2 selection, can also be found in three isolated cysteine-rich plant defensins

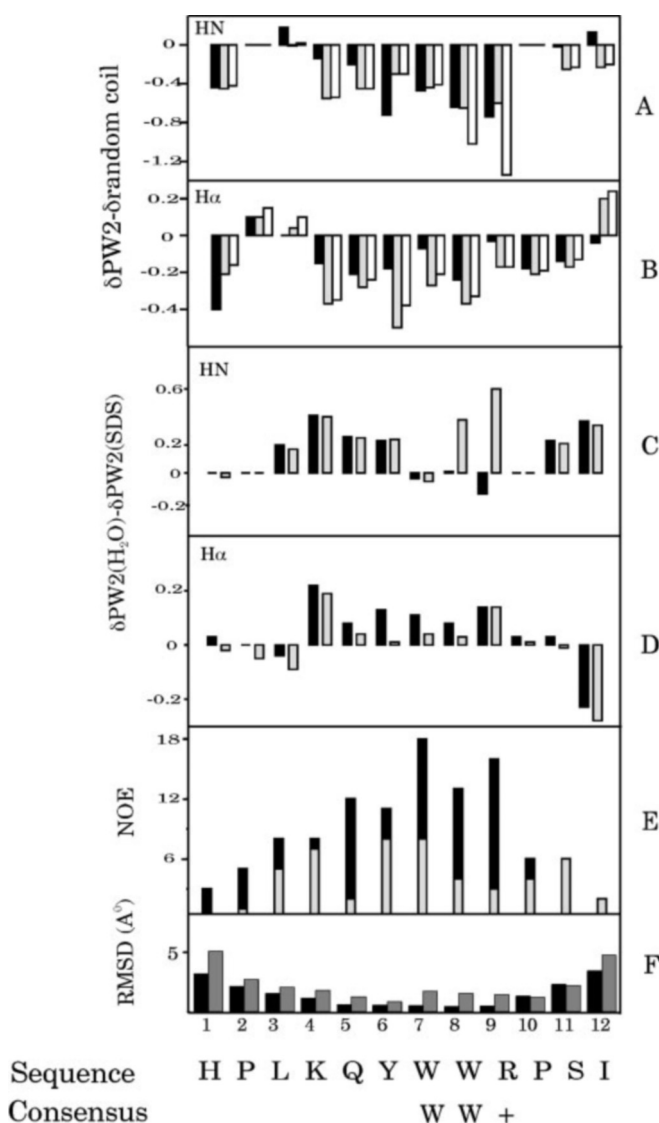


FIG. 4. **Summary of chemical shifts and structure data for PW2.** A, chemical shift differences between PW2 amidic hydrogens and the respective random coil values (33). *Black*, PW2 in 20 mM sodium phosphate buffer at pH 5.0; *gray*, SDS/PW2 molar ratio 10; *white*, SDS/PW2 molar ratio 40. B, chemical shift differences between PW2 α -hydrogens and the respective tabulated values for random coil. *Black*, PW2 in 20 mM sodium phosphate buffer at pH 5.0; *gray*, SDS/PW2 molar ratio 10; *white*, SDS/PW2 molar ratio 40. C, chemical shift differences between PW2 amidic hydrogens in 20 mM sodium phosphate buffer at pH 5.0 and in SDS. *Black*, SDS/PW2 molar ratio 10; *gray*, SDS/PW2 molar ratio 40. D, chemical shift differences between PW2 α -hydrogens in 20 mM sodium phosphate buffer at pH 5.0 and in SDS. *Black*, SDS/PW2 molar ratio 10; *gray*, SDS/PW2 molar ratio 40. E, number of non-ambiguous NOEs for residue used as distance constraints for the structure calculation of PW2 in SDS micelles. *Black*, total; *gray*, inter-residue. F, r.m.s.d. for amino acid residues calculated for the 20 lowest energy structures using the PROCHECK program (37). *Black*, backbone; *gray*, heavy.

(thionins) with antifungal and antibacterial activity *in vitro*. The Trp-rich domain of both puroindoline-a (WRWWKWWK) and puroindoline-b (WPTKWWK) present the consensus WW+ and, in the case of the antimicrobial protein ACE-AMP1 from onion seeds, the Trp-rich region (TFVRPFWWRPRI) (10, 34) displays high similarity with the sequence of PW2 (HPLKQY-WWRPSI). These proteins (puroindolines and Ace-AMP1), found in wheat and onion seeds, show sequence and structural similarities with the family of the nonspecific lipid transport proteins (nsLTPs) but are unable to transfer phospholipids between vesicles or organelles *in vitro*. Nevertheless, these

proteins are able to bind to polar phospholipids, increasing the permeability of model membranes (10, 11, 34, 35) as observed for the Trp-rich antimicrobial peptides indolicidin and tritrpticin (5, 9).

The function of puroindolines *in vivo* is still unknown, but their *in vitro* antifungal and antibacterial activities together with the localization of the proteins in the aleurone of the seeds suggest that they play an important role in the protection of the seed (11, 35). Structural studies revealed that puroindolines and Ace-AMP1 present tryptophan residues that are exposed to the solvent. These are probable effectors in the binding and permeabilization of membranes (34, 35). In fact, exposed tryptophan residues are important for the activity of diverse membrane-disturbing toxins present in animal venoms (36). The three-dimensional structures of Trp-rich antimicrobial peptides (indolicidin and tritrpticin) also present solvent-exposed tryptophan residues (8, 9), which is also the case for PW2, as revealed by the present study.

Acknowledgment—We thank Prof. Franklin D. Rumjanek for revision.

REFERENCES

1. Zasloff, M. (2002) *Nature* **415**, 389–395
2. Silva, A. Jr., Kawazoe, U., Freitas, F. F. T., Gatti, M. S. V., Dolder, H., Shumacher, R. I., Juliano, M. A., Silva, M. J., and Leite, A. (2002) *Mol. Biochem. Parasitol.* **120**, 1, 53–60
3. Selsted, M. E., Novotny, M. J., Morris, W. L., Tang, Y. Q., Smith, W., and Cullor, J. S. (1992) *J. Biol. Chem.* **267**, 4292–4295
4. Aley, S. B., Zimmerman, M., Hetsko, M. Selsted, M. E., and Gillin, F. D. (1994) *Infect. Immun.* **62**, 5397–5403
5. Ahmad, I., Perkins, W. R., Lupan, D. M. Selsted, M. E., and Janoff, A. S. (1995) *Biochim. Biophys. Acta* **1237**, 109–114
6. Robinson, W. E., Jr., McDougall, B., Tran, D., and Selsted, M. E. (1998) *J. Leukocyte Biol.* **63**, 94–100
7. Lawyer, C. Pai, S., Watabe, M., Borgia, P., Mashimo, T., Eagleton, L., and Watabe, K. (1996) *FEBS Lett.* **390**, 95–95
8. Rozek, A., Friedrich, C. L., and Hancock, R. E. W. (2000) *Biochemistry* **39**, 15765–15774
9. Schibli, D. J., Hwang, P. M., and Vogel, H. J. (1999) *Biochemistry* **38**, 16749–16755
10. Cammue, B. P. A., Thevissen, K., Hendriks, M., Eggermont, K., Goderis, I. J., Proost, P., Van Damme, J., Osborn, R. W., Guerbet, F., Kader, J. C., and Broekaert, W. F. (1995) *Plant Physiol.* **109**, 445–455
11. Le Bihan, T., Blochet, J. E., Desormeaux, A., Marion, D., and Pezolet, M. (1996) *Biochemistry* **35**, 12712–12722
12. Wu, M., Maier, E., Benz, R., and Hancock, R. E. (1999) *Biochemistry* **38**, 7235–7242
13. Matsuzaki, K. (1999) *Biochim. Biophys. Acta* **1462**, 1–10
14. Yang, L. Weiss, T. M. Lehrer, R. I., and Huang, H. W. (2000) *Biophys. J.* **79**, 2002–2009
15. Shai, Y. (1999) *Biochim. Biophys. Acta* **1462**, 55–70
16. Subbalakshmi, C. Krishnakumari, V., Nagaraj, R., and Sitaram, N. (1996) *FEBS Lett.* **395**, 48–52
17. Friedrich, C. L., Rozek, A., Patrzykat, A., and Hancock, R. E. W. (2001) *J. Biol. Chem.* **276**, 24015–24022
18. Zhao, H., Mattila, J. P., Holopainen, J. M., and Kinnunen, P. K. J. (2001) *Biophys. J.* **81**, 2979–2991
19. Zhang, L., Rozek, A., and Hancock, R. E. W. (2001) *J. Biol. Chem.* **276**, 35714–35722
20. Westerhoff, H. V., Juretic, D., Hendler, R. W., and Zasloff, M. (1989) *Proc. Natl. Acad. Sci. U. S. A.* **86**, 6597–6601
21. Bierbaum, G., and Sahl, H. G. (1985) *Arch. Microbiol.* **141**, 249–254
22. Kragol, G. (2001) *Biochemistry* **40**, 3016–3026
23. Bax, A., and Davis, D. G. (1985) *J. Magn. Reson.* **65**, 355–360
24. Sklenar, V., Piotto, M., Leppeck, R., and Sandek, V. (1993) *J. Magn. Reson., Series A* **102**, 241–245
25. Piotto, M., Sandek, V., and Sklenar, V. (1992) *J. Biomol. NMR* **2**, 661–666
26. Delaglio, F., Grzesiek, S., Zhu, G., Vuister, G. W., Pfeifer, J., and Bax, A. (1995) *J. Biomol. NMR* **6**, 277–293
27. Johnson, B. A., and Blevins, R. A. (1994) *J. Biomol. NMR* **4**, 603–614
28. Hyberts, S. G., Goldberg, M. S. Havel, T. F., and Wagner, G. (1992) *Protein Sci.* **1**, 736–751
29. Brunger, A. T., Adams, P. D., Clore, G. M., Delano, W. L., Gros, P., Grosse-Kunstleve, R. W., Jiang, J. S., Kuszewski, J., Nilges, N., Pannu, N. S., Read, R. J., Rice, L. M., Simonson, T., and Warren, G. L. (1998) *Acta Crystallogr. Sect. D Biol. Crystallogr.* **54**, D905–D921
30. Koradi, R., Billeter, M., and Wüthrich, K. (1996) *J. Mol. Graphics* **14**, 51–55
31. Woody, R. W. (1994) *Eur. Biophys. J. Biophys.* **23**, 253–262
32. Yang, J. J. Pitkeathly, M., and Radford, S. E. (1994) *Biochemistry* **33**, 7345–7353
33. Wüthrich, K. (1986). *NMR of Proteins and Nucleic Acids*, Wiley-Interscience, New York
34. Tassin, S., Broekaert, W. F., Marion, D., Acland, D., Ptak, M., Vovelle, F., and Sodano, P. (1998) *Biochemistry* **37**, 3623–3637
35. Gautier, M. F., Joudrier, P., Pezolet, M., and Marion, D. (1993) *FEBS Lett.* **329**, 336–340
36. Gatineau, E., Thoma, F., Montenay-Garestier, Th., Takeshi, M., Fromageot, P., and Ménez, A. (1987) *Biochemistry* **26**, 8046–8055
37. Laskowski, R. A., Rullman, J. A. C., MacArthur, M. W., Kaptein, R., and Thornton, J. M. (1996) *J. Biomol. NMR* **8**, 477–486